Chemical Science

EDGE ARTICLE

View Article Online
View Journal | View Issue

Cite this: *Chem. Sci.*, 2015, **6**, 5284

Overcoming aggregation in indium salen catalysts for isoselective lactide polymerization†

D. C. Aluthge, J. M. Ahn and P. Mehrkhodavandi*

Received 1st May 2015
Accepted 20th June 2015

DOI: 10.1039/c5sc01584g

www.rsc.org/chemicalscience

A methodology for controlling aggregation in highly active and isoselective indium catalysts for the ring opening polymerization of racemic lactide is reported. A series of racemic and enantiopure dinuclear indium ethoxide complexes bearing salen ligands $[(ONNO_R)InOEt]_2$ (R = Br, Me, admantyl, cumyl, *t*-Bu) were synthesized and fully characterized. Mononuclear analogues $(ONNO_R)InOCH_2Pyr$ (R = Br, *t*-Bu, $SiPh_3$) were synthesized by controlling aggregation with the use of chelating 2-pyridinemethoxide functionality. The nuclearity of metal complexes was confirmed using PGSE NMR spectroscopy. Detailed kinetic studies show a clear initiation period for these dinuclear catalysts, which is lacking in their mononuclear analogues. The polymerization behavior of analogous dinuclear and mononuclear compounds is identical and consistent with a mononuclear propagating species. The isotacticity of the resulting polymers was investigated using direct integration and peak deconvolution methodologies and the two were compared.

Introduction

Poly (lactic acid) (PLA) is a biodegradable polyester[1] with increasing impact in emerging markets[2] and numerous commercial[3] and cutting edge scientific[4] applications. Attempts to extend this range of applications have focused on improving PLA macro-[5] and microstructure.[6] A major challenge in the field is the ring opening polymerization (ROP) of a mixture of lactide isomers to yield PLA with controlled mechanical properties. A benchmark study in this field is the site selective polymerization of racemic lactide (*rac*-LA) to form isotactic PLA. Although organo-[7] and metal catalysts[6] ranging the entire periodic table[8] have been evaluated for this reaction, only a few have generated highly isotactic PLA material.[9] Trivalent metals supported by salen[10] and phosphasalen[11] type ligands have been particularly successful. While aluminum catalysts have been prevalent in the literature,[6a] recent work by our group[12] and others[9f,h,13] shows that indium complexes have the potential to be more reactive and functional group tolerant than their aluminum analogues.

The majority of ROP catalysts are comprised of a chelate-supported Lewis acidic metal centre with an alkoxide initiator built in or generated *in situ via* alcoholysis.[1] Due to the electrophilicity of the metal centres and the bridging ability of the alkoxide ligands, aggregation is observed in many of these systems.[13h,l,14] While aggregation can be beneficial in some cases,[15] in others it can lead to poor control over catalyst speciation and reactivity, as well as polymer macro- and microstructure (Chart 1).[16] For example, dinuclear isopropoxide bridged β-diiminate magnesium complex **A**[16d] is not selective for the polymerization of *rac*-LA, while the mononuclear analogue **B**[17] is highly heteroselective. Aggregation impacts polymerization processes by generating competing active species, as observed for complex **C**.[16f] In our asymmetrically-bridged indium systems **D**, any disturbance of catalyst nuclearity leads to loss of stereoselectivity and complicates isolation of discrete complexes.[18] Similar studies on the role of steric effects on catalyst selectivity of aluminum salen complexes show that these trends are not entirely predictable.[10n] While the issue of aggregation persists in the literature, to the best of our knowledge no broadly applicable strategy has been put forward to overcome this challenge.

Aggregation phenomena are especially important for complexes bearing trivalent indium complexes due to their Lewis acidity and large ionic radii.[12b] In a recent communication, we reported a dinuclear indium salen alkoxide complex which is a highly active and isoselective catalyst for the ring-opening polymerization of racemic lactide at room temperature.[12a] Herein, we report our full investigations into the structure reactivity relationships of these catalysts, the aggregation phenomena we encountered, and the general strategy we developed to overcome aggregation in this system. We also investigate the isoselectivity of these systems in detail and discuss two different methods of quantifying P_m values for

Department of Chemistry, University of British Columbia, 2036 Main Mall, Vancouver, BC V6T 1Z1, Canada. E-mail: mehr@chem.ubc.ca

† Electronic supplementary information (ESI) available: Experimental section, full characterization of compounds in solution and in the solid state, polymerization and polymer analysis, details of reactivity, tacticity determination, DSC, PGSE studies, *in situ* polymerization studies. CCDC 1062730–1062733 and 1062738. For ESI and crystallographic data in CIF or other electronic format see DOI: 10.1039/c5sc01584g

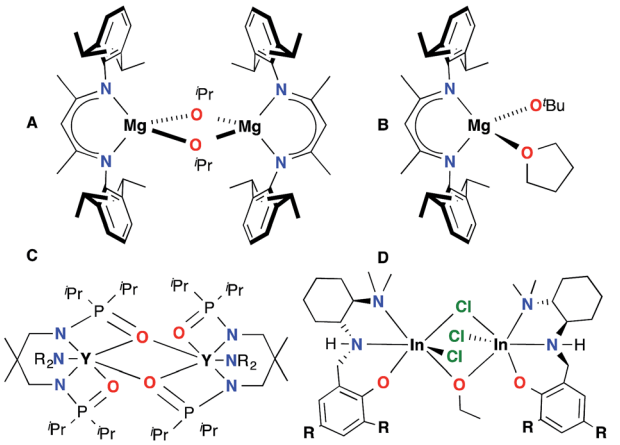

Chart 1 Some catalysts impacted by aggregation.

isotactic PLA. Finally, we discuss the nature of the propagating species and evaluate the efficacy of salen supports for indium complexes.

Results and discussion

Synthesis and characterization of complexes

Synthesis of proligands and indium chloride complexes. A series of tetradentate Schiff base salen ligands, (±)- or (*R*,*R*)-$H_2(ONNO_R)$, with various *ortho*-phenolate groups (R) can be synthesized by treating mono-(+)-tartrate salts of (±)-1,2-diaminocyclohexane or (*R*,*R*)-1,2-diammoniumcyclohexane with two equiv. of the corresponding salicylaldehydes under basic conditions.[19] The ^{1}H NMR spectra ($CDCl_3$, 25 °C) of all the proligands show one characteristic singlet between 8 and 9 ppm, which corresponds to the two equivalent N=C*H* resonances. In the corresponding $^{13}C\{^1H\}$ spectra, the N=*C*H resonances appear at >160 ppm.

Metallation reactions are ligand dependent and can be carried out *via* two routes. The first is deprotonation of the proligands followed by salt metathesis with an appropriate indium trihalide compound, as reported for (±)/(*R*,*R*)-**1** previously.[12a] Deprotonation of (±)/(*R*,*R*)-$H_2(ONNO_R)$ with two equiv. of KCH_2Ph or KO*t*-Bu, followed by addition of one equiv. of $InCl_3$, yields the respective racemic or enantiopure indium chloride derivatives (±)/(*R*,*R*)-$(ONNO_R)InCl$ (R = *t*-Bu **1**, Me **2**, Ad **3**, Cm **4**, $SiPh_3$ **5**) (Scheme 1). However, similar reactions with (*R*,*R*)-$H_2(ONNO_{Br})$ form intractable mixtures, necessitating a different synthetic route towards alkoxide complexes as described later in this work. The ^{1}H NMR spectra of complexes (±)/(*R*,*R*)-**1–5** show two singlet resonances corresponding to the N=C*H* group between 8 and 9 ppm, indicative of the loss of the C_2 rotational axis of the ligand after metallation. The ^{1}H NMR spectra of the racemic complexes are identical to their enantiopure analogues (Fig. S5–S12†).

The solid state structures of (±)-**1** [12a] and (±)-**3** (Fig. S39†), determined by single crystal X-ray crystallography, contain five-coordinate indium centers with unremarkable distorted square pyramidal geometries. In contrast, the structure of (*R*,*R*)-**2**·CH_3CN, obtained in acetonitrile, has a distorted octahedral geometry with an acetonitrile molecule coordinating to the indium *trans* to the chloride (Fig. S40†). The In–Cl distance in (*R*,*R*)-**2**·CH_3CN (Å) is longer than the In–Cl bond distances in either (±)-**1** or (±)-**3** (2.470(1), 2.371(2) and 2.3704(7) Å for **2**·CH_3CN, **1**, and **3** respectively) and can be attributed to the *trans* influence from the coordinating acetonitrile.

Synthesis of dimeric ethoxide-bridged indium complexes using salt metathesis. A salt metathesis strategy can be used in the formation of indium alkoxide complexes with relatively unhindered alkyl functionalized proligands. We have reported the salt metathesis reaction of complex **1** with limited amounts of NaOEt to yield (±)/(*R*,*R*)-$[(ONNO_{tBu})InOEt]_2$ (**6**).[12a] This methodology can be extended to complexes (*R*,*R*)-**2–4**, to generate (*R*,*R*)-**7–9**, respectively (Scheme 1). However, a similar reaction with $SiPh_3$-substituted (*R*,*R*)-**5** generates an intractable mixture of products. The ^{1}H NMR spectra of complexes (*R*,*R*)-**7–9** show two characteristic C=N*H* resonances, similar to those observed for the $(ONNO_R)InCl$ complexes. Compounds (*R*,*R*)-**6–8** contain two diastereotopic multiplet resonances for the $-OCH_2CH_3$ protons between 3 and 4 ppm, while in the spectrum of (*R*,*R*)-**9**, perhaps as a result of the increased steric hinderance,

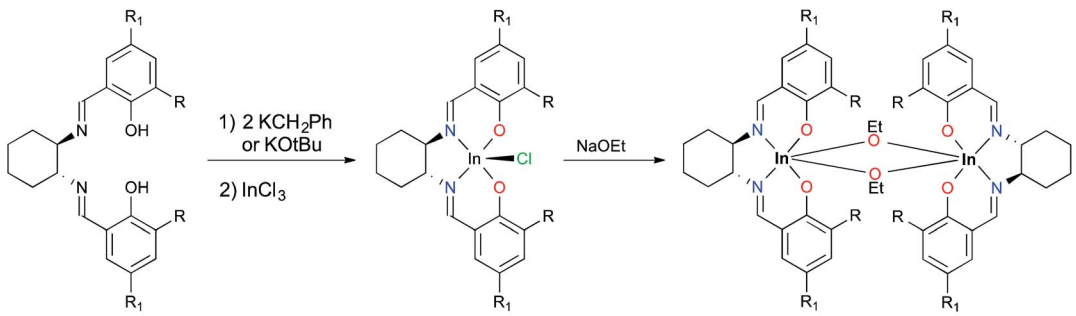

(±)/(*R*,*R*)-$H_2(ONNO_R)$
R_1 = *t*-Bu, Me, Cm

(±)/(*R*,*R*)-$(ONNO_{tBu})InCl$ (**1**)
(*R*,*R*)-$(ONNO_{Me})InCl$ (**2**)
(±)/(*R*,*R*)-$(ONNO_{Ad})InCl$ (**3**)
(*R*,*R*)-$(ONNO_{Cm})InCl$ (**4**)
(*R*,*R*)-$(ONNO_{SiPh3})InCl$ (**5**)

(±)/(*R*,*R*)-$[(ONNO_{tBu})InOEt]_2$ (**6**)
(*R*,*R*)-$[(ONNO_{Me})InOEt]_2$ (**7**)
(±)/(*R*,*R*)-$[(ONNO_{Ad})InOEt]_2$ (**8**)
(*R*,*R*)-$[(ONNO_{Cm})InOEt]_2$ (**9**)

Scheme 1 Synthesis of salen indium complexes **1–9**.

these methylene protons appear as a quartet at 3.51 ppm (Fig. S13–S18†).

The solid state molecular structure of (*R*,*R*)-**7**, determined by single crystal X-ray crystallography, is analogous to that of complex (±)-**6** (Fig. 1).[12a] Both complexes are dimeric, with distorted octahedral geometries around the indium centres and comparable bond lengths and angles. A notable difference between the structures of **6** and **7** is the distortion in the salen ligand despite the rigid cyclohexyl backbone. While 6-coordinate dimeric $[(salen)Al(OR)]_2$ complexes are known,[20] the most common coordination number for salen aluminum alkoxide complexes is five.[10o,21] In contrast, the larger ionic radius of In(III) often renders indium alkoxide complexes prone to aggregation and formation of dimeric $[(\kappa^4\text{-ligand})In(OR)]_2$ complexes such as those reported by us[12b] and others.[13l,21,22]

Synthesis of dimeric ethoxide-bridged indium complexes using a one-pot procedure. While the salt metathesis methodology works well with many ligands, it is not applicable to systems such as (*R*,*R*)-$H_2(ONNO_{Br})$ where isolation of the indium chloride complex is challenging. In order to access these indium alkoxide complexes, a one-pot strategy can be used.[15a] Stirring the $H_2(ONNO_R)$ proligands with $InCl_3$ forms preliminary adducts, which can then react with excess NaOEt to form the desired products (Scheme 2).[23] This milder procedure efficiently generates (*R*,*R*)-**6–10** from their respective proligands in 50–70% yields.

Synthesis of mononuclear indium salen alkoxide complexes. Indium salen alkoxide complexes bearing the bulkier $-SiPh_3$ group cannot be synthesized using either of the above strategies. We hypothesize that dimerization of indium alkoxide complexes is a necessary thermodynamic minimum, which prevents further aggregation and facilitates the formation of discrete compounds.[12b,18]

Replacement of the ethoxide group with a coordinating alkoxide, namely pyridin-2-ylmethoxide, solves this problem. This approach affords an indium–alkoxide bond where the pyridine moiety can occupy the final coordination site to form a stable six-coordinate metal center. Complexes (*R*,*R*)-**11** and (*R*,*R*)-**12** can be prepared using the salt metathesis route by treating (*R*,*R*)-**1** and (*R*,*R*)-**5**, respectively, with potassium pyridin-2-ylmethoxide, $KOCH_2Pyr$ (Scheme 3). The *ortho*-bromo complex can be accessed in a one-pot synthesis by treating $H_2(ONNO_{Br})$ with $InCl_3$ and excess $KOCH_2Pyr$ (Scheme 3). In contrast to (*R*,*R*)-**11** and (*R*,*R*)-**13**, the bulkier complex (*R*,*R*)-**12** is more challenging to obtain in pure form, with minor impurities (~5–10%) observed by ^{1}H NMR spectroscopy after repeated purification attempts (Fig. S26†).

Single crystals of (*R*,*R*)-**11** and (*R*,*R*)-**12** can be obtained by slow evaporation from hexanes. The solid state structures of these mononuclear complexes show distorted octahedral indium centers supported by a chelating pyridyl moiety (Fig. 2). Comparison of the In–N bond distances of (*R*,*R*)-**11** shows that the In–NPyr bond distance of 2.296(2) Å is longer than the two In–NImine bond distances (2.228(2) and 2.258(2) Å). In contrast, for (*R*,*R*)-**12** the In–N bond distances have similar values, with In–NPyr and the two In–NImine being 2.242(7), 2.233(7), and 2.234(6) Å, respectively. The shorter In–NPyr bond for (*R*,*R*)-**12** indicates stronger coordination of the pyridyl moiety. The C–Si bond distances (1.862(8)–1.874(8) Å) between the salicylaldehyde moiety and the $-SiPh_3$ groups are considerably longer than the analogous C–C bond distances in (*R*,*R*)-**11** (1.548(3)–1.539(3) Å), indicating that the steric bulk lies further away from the indium centre in (*R*,*R*)-**12** compared to (*R*,*R*)-**11**.

The solution structures of these compounds correspond to those in the solid state. The ^{1}H NMR spectra of (*R*,*R*)-**11** and (*R*,*R*)-**13** show singlets corresponding to the methylene resonances of pyridin-2-ylmethoxide at 5.03 and 4.77 ppm, respectively (Fig. S22–S27†). However in (*R*,*R*)-**12**, with the bulkier $-SiPh_3$ groups, the methylene protons appear as two diastereotopic resonances at 4.59–4.54 and 4.05–4.01 ppm. This

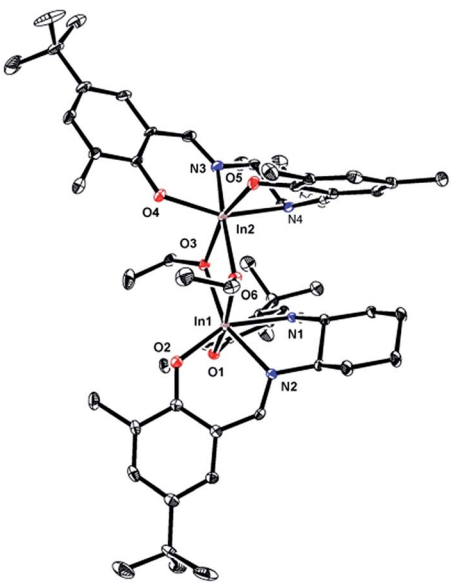

Fig. 1 Molecular structure of (*R*,*R*)-**7** depicted with ellipsoids at 50% probability (H atoms and solvent molecules omitted for clarity).

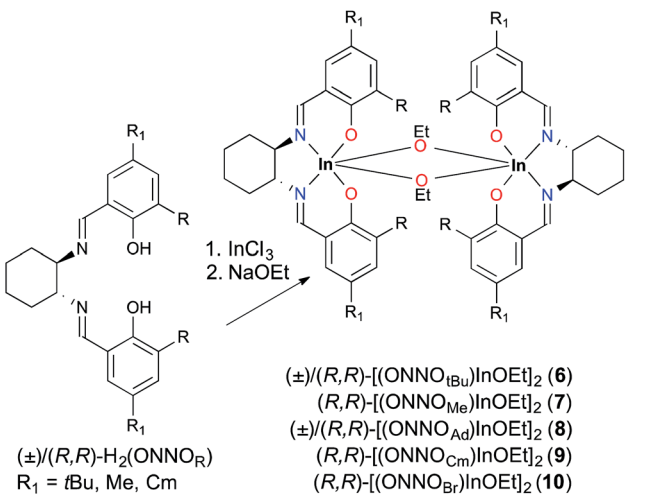

Scheme 2 One-pot synthesis of complexes **6–10**.

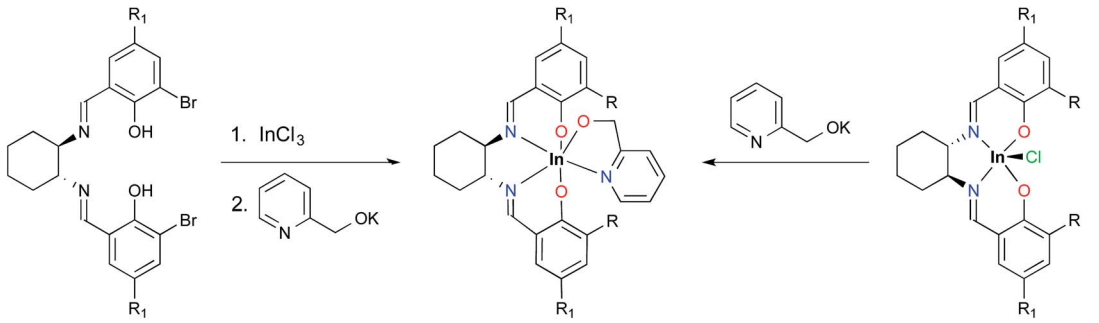

Scheme 3 Synthesis of (*R*,*R*)-(ONNO$_R$)InOCH$_2$Pyr complexes.

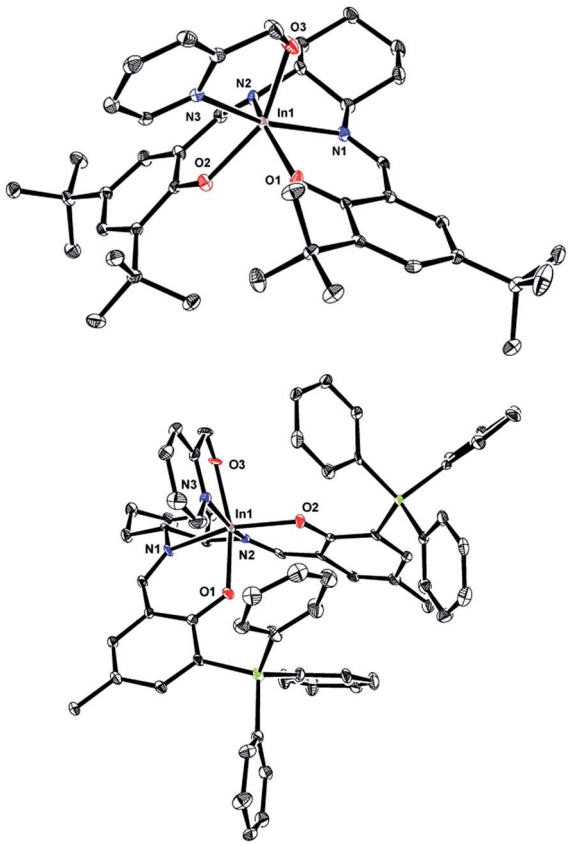

Fig. 2 (A) (top) Molecular structure of (*R*,*R*)-**11** depicted with ellipsoids at 50% probability (H atoms and solvent molecules omitted for clarity) (B) (bottom) Molecular structure of (*R*,*R*)-**12** depicted with ellipsoids at 50% probability (H atoms omitted for clarity).

suggests fluxional behaviour of the pyridine moiety in (*R*,*R*)-**11** and (*R*,*R*)-**13**, which is hindered in **12**. Variable temperature ^{1}H NMR spectra ($CDCl_3$) of (*R*,*R*)-**11** show the room temperature singlet at 5.03 ppm resolving into two diastereotopic resonances at −20 °C (Fig. S31†).

Solution structures of salen indium alkoxide complexes. We have shown that the nuclearity of indium complexes can have a significant impact on their reactivity and selectivity in lactide polymerization.[15a,c,18] Previously, we determined that complex **6** is dinuclear in solution by using diffusion coefficient determined using Pulsed Gradient Spin Echo (PGSE) NMR spectroscopy.[12a] Using the same methodology (Fig. S51†), we can obtain the diffusion coefficients (D_t) for complexes **7**–**11** and **13** and compare them to the D_t values of species with known solution structures (Table 1). The D_t values of the ethoxide-bridged complexes **6**–**10** are similar, with values 20–30% smaller than those for the proligands, confirming the dinuclear nature of these complexes (Table 1, entries 5–9). In contrast, complexes **11** and **13** have D_t values similar to those of the proligand and of complex (±)-**1**, which indicates that these complexes remain mononuclear in solution (Table 1, entries 3–4).

The alkoxide-bridged dimers have different stabilities in solution, which can affect their reactivity with lactide. The ^{1}H NMR spectrum of (*R*,*R*)-**6** in THF-d_8 shows no indication of dissociation. When (*R*,*R*)-**6** is stirred in refluxing pyridine for 16 h no changes in the complex are observed in the ^{1}H NMR spectrum (Fig. S29†). However, a similar reaction in neat ethyl

Table 1 Diffusion constants and hydrodynamic radii of compounds calculated using PGSE NMR spectroscopy

	Compound	D_t[a] ($\times 10^{-10}$ m^2 s^{-1})	r_H[b]	$r_{X\text{-ray}}$[c]
1	H_2(ONNO$_{tBu}$)[24]	9.5(3)	6.1	5.9
2	(ONNO$_{tBu}$)InCl (±)-**1** [12a]	9.1(2)	6.4	5.9
3	(ONNO$_{Br}$)InOCH$_2$Pyr (*R*,*R*)-**13**	8.6(5)	6.6	—
4	(ONNO$_{tBu}$)InOCH$_2$Pyr (*R*,*R*)-**11**	8.5(2)	6.7	6.2
5	[(ONNO$_{Br}$)InOEt]$_2$ (*R*,*R*)-**10**	6.9(4)	8.1	—
6	[(ONNO$_{Me}$)InOEt]$_2$ (*R*,*R*)-**7**	7.0(4)	8.0	7.8
7	[(ONNO$_{tBu}$)InOEt]$_2$ (±)-**6** [12a]	6.5(5)	8.5	8.3
8	[(ONNO$_{Ad}$)InOEt]$_2$ (*R*,*R*)-**8**	6.3(5)	8.8	—
9	[(ONNO$_{Cm}$)InOEt]$_2$ (*R*,*R*)-**9**	6.0(4)	9.2	—

[a] D_t was determined using PGSE NMR spectroscopy with tetrakis(trimethylsilyl)silane (TMSS) as an internal standard. [Compound] = 4.5 mM samples were prepared in 0.94 mM TMSS solution in CD_2Cl_2. D_t is calculated from slopes of plots of $\ln(I/I_0)$ *vs.* $\gamma^2\delta^2G^2[\Delta - (\delta/3)] \times 10^{-10}$ (m^2 s^{-1}). [b] Calculated from D_t values using a modified Stokes–Einstein equation (see ESI). [c] Calculated, where solid-state data is available, from the crystal structure unit cell volume (V) as well as the number of the compound of interest (n) occupying the unit cell assuming spherical shape $(3V/4\pi n)^{1/3}$.

acetate shows that ~20% of the compound is converted to other products (Fig. S30†). This suggests that while the dinuclear ethoxide complex is stable in solution, it can dissociate in the presence of esters like ethyl acetate and lactide.

The relative stability of these complexes can be investigated further by using crossover experiments between the *t*-butyl substituted complex, (*R*,*R*)-**6**, and the adamantyl, and bromo-substituted analogues (*R*,*R*)-**8** and (*R*,*R*)-**10**, respectively. Notably, the (*R*,*R*)-**6**/(*R*,*R*)-**8** pair with bulkier *ortho* substituents shows almost complete crossover in 10 min (Fig. S32†) while the (*R*,*R*)-**6**/(*R*,*R*)-**10** pair shows no evidence of a crossover product in this period and only minor crossover after 16 h (Fig. S33†). This suggests that $[(ONNO_{Br})In(OEt)]_2$ is less prone to dissociation than the bulkier analogues.

Lactide polymerization studies

Impact of ligand substituents on selectivity. With the range of steric bulks on this family of indium salen complexes in hand, we can investigate the impact of the steric bulk of ligand substituents on the isoselective polymerization of racemic lactide (*rac*-LA) (Table 2). Gel permeation chromatographic (GPC) analysis of the polymers generated with catalysts (*R*,*R*)-**7**–**12** show good to excellent molecular weight control. Polymer dispersities are similar to those obtained for (*R*,*R*)-**6** and indicate significant transesterification.[12a] Polymerization reactions that are not quenched after full conversion can undergo depolymerization, which affects the molecular weights and PDIs. If an isolated polymer is redissolved and stirred for 16 h at room temperature along with (*R*,*R*)-**6**, a 30% decrease in the molecular weight is observed (Table S1†).

The catalysts in this family are isoselective. The P_m values can be calculated by substituting integrations of tetrad sequences, determined using $^1H\{^1H\}$ NMR spectroscopy (Fig. S44–S50†). The tacticity of PLA is calculated using a set of equations derived using a Bernoullian statistical model.[16d,25] While the use of these equations in the direct interpretation of integrations of $^1H\{^1H\}$ NMR spectra of PLA is well established,[26] other reports use the subtly different methodology of peak deconvolution for calculating tacticity.[9m,10s,11,26a,27] This issue has arisen partly due to the fact that with most commonly available NMR instruments, the mmr, mmm, mrm resonances overlap and cannot be integrated separately. Hence, calculation of P_m values can be based on the integration of rmr and rmm resonances in the majority of systems where perfectly isotactic PLA is not formed and stereoerrors are present (Method A) (see ESI†).

The accuracy of the P_m values calculated using deconvoluted spectra depends on the accuracy and the applicability of the deconvolution algorithm and spectral resolution. We encountered the limitations of this methodology in our systems. Inspection of the results in Table 2 shows that the deconvolution methodology has inflated the P_m values. In particular, inspection of entries 1 and 3 shows that catalysts **6** and **8** have nearly identical P_m values generated from Method A, while they have significantly different values from Method B. The discrepancy widens when comparing entries 3 and 5, with identical values for Method B and significantly different values for Method A.

Another inconsistency arises from the relationship between P_m and P_r values in this methodology. The most general form of the equations uses P_m and P_r as two independent variables, requiring the use of at least two different equations to calculate the tacticity.[16d,25] However, in order to apply method B the relationship $P_m = 1 - P_r$ must be true. In this case, these equations are reduced to expressions containing a single variable P_m values for each of the five resonances are calculated and

Table 2 Polymerization of *rac*-lactide with indium salen complexes

	Catalyst[a]	*M* : *I*	Time (h)	Conv[b] (%)	M_{ntheo} (kDa)	M_{nGPC}[c] (kDa)	*Đ*	P_m[d]	P_m[e]
1	$[(ONNO_{tBu})InOEt]_2$ (*R*,*R*)-**6**	200	1	99	28.5	34.9	1.39	0.76	0.85
2	$[(ONNO_{tBu})InOEt]_2$ (*R*,*R*)-**6**	600	4	99	85.5	89.5	1.52	0.75	—
3	$[(ONNO_{Ad})InOEt]_2$ (*R*,*R*)-**8**	200	1	98	28.2	36.3	1.42	0.77	0.80
4	$[(ONNO_{Ad})InOEt]_2$ (*R*,*R*)-**8**	500	2	99	71.3	69.4	1.33	0.74	—
5	$[(ONNO_{Cm})InOEt]_2$ (*R*,*R*)-**9**	200	2	97	27.9	27.9	1.56	0.73	—
6	$[(ONNO_{Cm})InOEt]_2$ (*R*,*R*)-**9**	500	5	98	70.6	79.0	1.42	0.72	0.80
7	$[(ONNO_{Br})InOEt]_2$ (*R*,*R*)-**10**	200	2	97	27.9	52.9	1.15	0.55	—
8	$[(ONNO_{Br})InOEt]_2$ (*R*,*R*)-**10**	500	5	99	71.3	97.0	1.35	0.57	0.70
9	$[(ONNO_{Me})InOEt]_2$ (*R*,*R*)-**7**	200	2	98	28.2	47.5	1.19	0.60	—
10	$[(ONNO_{Me})InOEt]_2$ (*R*,*R*)-**7**	500	5	99	71.3	91.7	1.29	0.62	0.71
11	$(ONNO_{tBu})InOCH_2Pyr$ (*R*,*R*)-**11**	200	1	98	28.5	36.7	1.27	0.74	0.78
12	$(ONNO_{tBu})InOCH_2Pyr$ (*R*,*R*)-**11**	600	4	97	83.5	86.1	1.37	0.75	—
13	$(ONNO_{Br})InOCH_2Pyr$ (*R*,*R*)-**13**	200	0.5	98	28.2	35.8	1.15	0.59	0.69
14	$(ONNO_{Br})InOCH_2Pyr$ (*R*,*R*)-**13**	500	0.5	98	70.6	70.4	1.25	0.56	—
15	$(ONNO_{SiPh_3})InOCH_2Pyr$ (*R*,*R*)-**12**	200	16	75	—	—	—	0.73	—
16	$(ONNO_{SiPh_3})InOCH_2Pyr$ (*R*,*R*)-**12**	200	24	93	26.8	36.7	1.30	0.75	—

[a] In CH_2Cl_2 at 25 °C, [catalyst] ≈ 1 mM. [b] Conversions were determined by ^1H NMR spectroscopy. M_{ntheo} = molecular weight of chain-end + 144 g mol^{-1} × 200 × conversion. [c] In THF (2 mg mL^{-1}) and molecular weights were determined by GPC-LLS (flow rate = 0.5 mL min^{-1}). Universal calibration was carried out with polystyrene standards, laser light scattering detector data, and concentration detector. Each experiment is duplicated to ensure precision. [d] Calculated according to Method A, using the relative integrals of rmr and rmm resonances (see ESI). [e] Calculated using Method B after performing peak deconvolution to integrate all five peaks in the methine region of $^1H\{^1H\}$NMR spectra (see ESI).

averaged to give the final P_m value of the polymer.[26a] This derivation, however, is only valid for a system with exclusive site control where a single statistical event does not impact the other, not for those where both site and chain-end control may be operative such as the system under investigation here.[25]

While we acknowledge that there is no ideal way to calculate tacticities based on these equations due to the non-ideal behaviour of natural systems, we conclude that a comparison of P_m values obtained using the two different methods of calculation is precarious. We do not claim one method to be superior to the other; however, any comparison of literature P_m values must be carried out with consistency and transparency. In particular, Method B does not account well for systems where chain end control may be a significant contributor to selectivity such as ours.

Polymer melting point is a stronger arbiter of isotacticity in PLA. In our systems, the polymers generated from *rac*-LA with most stereoselective catalysts, (*R*,*R*)-**6** and (*R*,*R*)-**8**, are amorphous ($T_g \sim 55$ °C) (Fig. S37 and S38†). In comparison, Williams *et al.* have reported polymers with similar P_m values obtained using peak deconvolution methodology which are crystalline and have T_m values > 170 °C. Clearly, a comparison of the two systems using only the P_m values obtained using peak deconvolution is insufficient.[11]

A comparison of the selectivities listed in Table 2 using Method A shows that a decrease in ligand steric hinderance correlates to decreased P_m values, while increasing the steric bulk of the ligands does not result in appreciable increase in P_m values above ~0.75. A similar observation was made by Carpentier *et al.* in a series of aluminum salen catalysts with a chiral diphenyl ethylene backbone for lactide polymerization, where changing the *ortho* substituent from *t*-butyl group to a methyl functionality decreased the isoselectivity from P_m ~0.9 to ~0.8.[10s] This suggests that, although the *ortho* substituents of the salicylaldehyde moieties play a key role in imparting stereoselectivity, the mechanism for control of selectivity may be more nuanced.

The differences in ligand steric bulk have a significant impact on rates of propagation. The cumyl-substituted complex (*R*,*R*)-**9** requires longer reaction times for reaching full conversion than adamantyl substituted (*R*,*R*)-**8** under the same reaction conditions. This may be due to a more sterically congested ligand environment, which hinders the approach of lactide to the metal centre. *In situ* monitoring of catalysts (*R*,*R*)-**8** and (*R*,*R*)-**9** shows first order rates for the ring opening polymerization of L-, D-, and *rac*-LA similar to those observed for (*R*,*R*)-**6** (Fig. S52†). The plot for (*R*,*R*)-**8** shows a brief initiation period followed by linear propagation, while for (*R*,*R*)-**9** the initiation period is not observable. Both catalysts polymerize L-LA more rapidly than D-LA, with $k_{L\text{-}LA}/k_{D\text{-}LA}$ values of 4 and 6, respectively, for (*R*,*R*)-**8** and (*R*,*R*)-**9** (Table 3, entries 1, 2 and 4, 5).

Aside from the loss of isotactic bias discussed earlier, a closer examination of the polymerization behaviour of $[(ONNO_{Br})InOEt]_2$ (*R*,*R*)-**10** and $[(ONNO_{Me})InOEt]_2$ (*R*,*R*)-**7** can elucidate the impact of decreased steric bulk on reaction rates (Table 2, entries 7–10). Counter-intuitively, both (*R*,*R*)-**10** and (*R*,*R*)-**7** polymerize 200 equiv. of *rac*-LA in double the time required for the bulkier (*R*,*R*)-**6** under identical conditions. Furthermore, catalysts **7** and **10** are unique in the series for generating polymers with higher than expected molecular weights at low monomer loading (Table 2, entries 7 and 9).

Table 3 Rate constants for polymerization of D-, L-, and *rac*-LA with (*R*,*R*)-**8**, (*R*,*R*)-**9**, (*R*,*R*)-**11** and (*R*,*R*)-**13**[a]

	Catalyst[a]	M[b]	k_{obs} ($\times 10^{-4}$ s^{-1})
1	$[(ONNO_{Ad})InOEt]_2$ (*R*,*R*)-**8**	D-LA	9.4(2)
2	$[(ONNO_{Ad})InOEt]_2$ (*R*,*R*)-**8**	L-LA	38(8)
3	$[(ONNO_{Ad})InOEt]_2$ (*R*,*R*)-**8**	*rac*-LA	9.4(2)
4	$[(ONNO_{Cm})InOEt]_2$ (*R*,*R*)-**9**	D-LA	2.4(5)
5	$[(ONNO_{Cm})InOEt]_2$ (*R*,*R*)-**9**	L-LA	14(3)
6	$[(ONNO_{Cm})InOEt]_2$ (*R*,*R*)-**9**	*rac*-LA	2.7(5)
7	$(ONNO_{tBu})InOCH_2Pyr$ (*R*,*R*)-**11**	D-LA	6.1(12)
8	$(ONNO_{tBu})InOCH_2Pyr$ (*R*,*R*)-**11**	L-LA	29(6)
9	$(ONNO_{tBu})InOCH_2Pyr$ (*R*,*R*)-**11**	*rac*-LA	6.9(14)
10	$(ONNO_{Br})InOCH_2Pyr$ (*R*,*R*)-**13**	D-LA	53(11)
11	$(ONNO_{Br})InOCH_2Pyr$ (*R*,*R*)-**13**	L-LA	52(10)
12	$(ONNO_{Br})InOCH_2Pyr$ (*R*,*R*)-**13**	*rac*-LA	62(12)

[a] All reactions were carried out with 200 equiv. of monomer (M) in CD_2Cl_2 at 25 °C and followed to 90% conversion by ^1H NMR spectroscopy. [a][Catalyst] = 0.0011 M, [b][M] = 0.45 M.

In situ monitoring of catalysts (*R*,*R*)-**7** and (*R*,*R*)-**10** shows that the rates of polymerization of *rac*-LA for these catalysts do not have a first order dependence on lactide concentration (Fig. S53†). First order plots for the polymerization of L-, D- and *rac*-LA with both catalysts show long initiation periods (>1 h) compared to (*R*,*R*)-**6**, with (*R*,*R*)-**10**. This is consistent with the higher than expected molecular weights of the polymers. While first order rate constants cannot be calculated due to the curved nature of the plots, a qualitative assessment of the plots asserts that (*R*,*R*)-**10** does not show a marked preference for one enantiomer of lactide over the other. This is consistent with the essentially atactic nature of the polymers generated ($P_m \sim 0.55$). Complex (*R*,*R*)-**7**, which generates PLA with modest isotacticity ($P_m \sim 0.60$), shows a higher rate for the polymerization of L-LA. These observations, in conjunction with the much shorter initiation periods observed for the bulkier complexes (*R*,*R*)-**6**, (*R*,*R*)-**8**, and (*R*,*R*)-**9**, suggest that the bulkier complexes undergo more facile initiation.

Nature of the propagating species. Although complexes **6–10** are dinuclear in solution, there is an equilibrium between the dimeric and monomeric forms which can be perturbed with addition of donors such as ethyl acetate (see above). This equilibrium may also be perturbed in the presence of lactide. In previous work with asymmetrically-bridged dinulcear indium complexes supported by tridentate ligands, we showed that the propagating species in the presence of lactide is dinuclear[15c] and that the nuclearity of the propagating species is consequential in controlling the macro- and microstructure of PLA generated with these catalysts.[18] Thus, we need to determine the nuclearity of the propagating species to determine the mechanism of polymerization and the origin of the initiation period in the indium salen systems. We can hypothesize that if a

dinuclear complex $[(ONNO_R)In(OEt)]_2$ and its mononuclear analogue $(ONNO_R)InOCH_2Pyr$ show the same reactivity and selectivity, they share the same propagating species.

Polymerization data for $[(ONNO_{tBu})In(OEt)]_2$ (*R*,*R*)-**6**[12a] and $(ONNO_{tBu})InOCH_2Pyr$ (*R*,*R*)-**11** are nearly identical (Table 2, entries 1, 2 and 11, 12). Both complexes show living behaviour for polymerization of *rac*-LA (Fig. S36†). Polymers generated with both systems are isotactically enriched, with P_m values of ~0.75. The MALDI–TOF spectra of PLA oligomers made with both catalysts show peaks corresponding to $[H(C_3H_4O)_n(OZ)H]^+$ (Z = OEt or OCH_2Pyr) separated by $m/z \sim 72$, which indicates extensive transesterification (Fig. S34 and S35). The k_{obs} values and $k_{L\text{-}LA}/k_{D\text{-}LA}$ ratios (both 5) are consistent for (*R*,*R*)-**6** and (*R*,*R*)-**11** having the same propagating species (Fig. S54a†).

The only difference between complexes **6** and **11** is in the slight initiation period observed for **6**, which is not observed for **11** (Fig. S52a and S54a†). This distinction is magnified for the less bulky complexes $(ONNO_{Br})InOCH_2Pyr$ (*R*,*R*)-**13** and $[(ONNO_{Br})InOEt]_2$ (*R*,*R*)-**10**. Mononuclear complex (*R*,*R*)-**13** lacks the prolonged initiation period of its dinuclear analogue completely (Fig. S54b†) and is more active than any of the indium salen catalysts investigated in the series (Table 3, entries 10–12). Unlike (*R*,*R*)-**10**, the molecular weights of polymers made with (*R*,*R*)-**13** at low lactide loadings match the expected values closely (Table 2, entries 7 and 13), which is consistent with the lack of initiation period. Complexes (*R*,*R*)-**10** and **13** show no preference for either enantiomer of lactide and the polymers generated with both catalysts are essentially atactic; indicating that the initiation period does not affect overall selectivity (Table 2, entries 13 and 14).

We propose a mechanism where in the initiation step, dinuclear complexes dissociate in the presence of lactide to form mononuclear propagating species (Scheme 4). The equilibria between the monomeric and dimeric forms of the catalysts are dictated by the steric bulk of the ligand substituents. The initiation periods are longer for the less bulky dinuclear complexes **7** and **10** in comparison to complexes **6** and **8**. The bulkier cumyl-substituted dimer **9** does not have an observable initiation period. When mononuclear catalysts **11** and **13** are used, the initiation periods are also not observable, confirming that the initiation period is caused by the monomer–dimer equilibrium and that the active species are mononuclear.

Once aggregation is eliminated, the propagation rates for the mononuclear catalysts are entirely dependent on the ligand steric environment. The sterically bulky complex $(ONNO_{SiPh_3})InOCH_2Pyr$ (*R*,*R*)-**12** is the least active catalyst in this series of compounds and achieves >90% conversion in 24 hours (Table 2, entries 15 and 16). In contrast, $(ONNO_{Br})InOCH_2Pyr$ (*R*,*R*)-**13**, with the lowest steric bulk, has the highest reaction rate. This disparity can be attributed to the bulky *ortho*-phenolate groups hindering the reactivity of the monomer with the metal center. The decrease in rate does not affect selectivity; catalyst (*R*,*R*)-**12** generates isotactic PLA with $P_m \sim 0.75$.

The similarity in the isoselectivity of complexes **11** and **12** can be explained by examining the structures of the mononuclear complexes, as these are the propagating species (Fig. 2). It is clear that the coordination environment around the indium

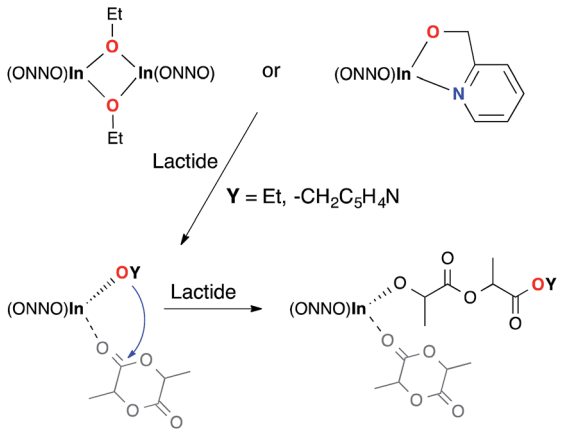

Scheme 4 Proposed initiation mechanism.

centres is flexible, and instead of generating a C_2 symmetric axis, the ligand creates a C_1 symmetric steric environment that prevents steric control of lactide coordination to the indium centres. In contrast, isoselective indium catalysts bearing tridentate half salen ligands (Chart 1D) remain dinuclear during propagation, highlighting the ligand-dependence of nuclearity in these indium based catalysts.

Conclusions

We investigated the structure/activity relationship for a series of dinuclear and mononuclear indium salen complexes. We showed that these complexes are excellent catalysts for the isoselective polymerization of racemic lactide.[28] In particular, we developed a generally applicable methodology for preventing aggregation in these systems by using a coordinating alkoxide, pyridin-2-ylmethoxide.[29] These mononuclear catalysts showed no initiation period and allowed us to determine that, unlike their tridentate counterparts, the propagating species for tetradentate indium salen complexes is mononuclear.

Although these clearly-defined mononuclear indium complexes allowed us to explore the effects of ligand substituents with a range of steric bulk on isoselective polymerization of lactide, we determined that the large ionic radius of indium allows for a great deal of flexibility in the structure and creates a ceiling for isoselective polymerization of racemic lactide. Our future efforts will be aimed at developing a new generation of ligand supports for indium.

Acknowledgements

PM gratefully acknowledges financial support from NSERC Strategic Grant and from Green Centre Canada.

Notes and references

1 O. Dechy-Cabaret, B. Martin-Vaca and D. Bourissou, *Chem. Rev.*, 2004, **104**, 6147–6176.
2 M. McCoy, *Chem. Eng. News*, 2014, **92**, 14.

3 G. Q. Chen and M. K. Patel, *Chem. Rev.*, 2012, **112**, 2082–2099.

4 C.-F. Cheng, H.-Y. Hsueh, C.-H. Lai, C.-J. Pan, B.-J. Hwang, C.-C. Hu and R. M. Ho, *NPG Asia Mater.*, 2015, **7**, e170.

5 (*a*) S. Corneillie and M. Smet, *Polym. Chem.*, 2015, **6**, 850–867; (*b*) M. Y. Xiong, D. K. Schneiderman, F. S. Bates, M. A. Hillmyer and K. C. Zhang, *Proc. Natl. Acad. Sci. U. S. A.*, 2014, **111**, 8357–8362; (*c*) M. A. Hillmyer and W. B. Tolman, *Acc. Chem. Res.*, 2014, **47**, 2390–2396; (*d*) A. L. Holmberg, K. H. Reno, R. P. Wool and T. H. Epps, *Soft Matter*, 2014, **10**, 7405–7424; (*e*) R. Roux, C. Ladaviere, A. Montembault and T. Delair, *Mater. Sci. Eng., C*, 2013, **33**, 997–1007; (*f*) K. Kataoka, A. Harada and Y. Nagasaki, *Adv. Drug Delivery Rev.*, 2012, **64**, 37–48; (*g*) J. K. Oh, *Soft Matter*, 2011, **7**, 5096–5108; (*h*) H. Z. Liu and J. W. Zhang, *J. Polym. Sci., Part B: Polym. Phys.*, 2011, **49**, 1051–1083.

6 (*a*) P. J. Dijkstra, H. Z. Du and J. Feijen, *Polym. Chem.*, 2011, **2**, 520–527; (*b*) J. C. Buffet and J. Okuda, *Polym. Chem.*, 2011, **2**, 2758–2763; (*c*) C. M. Thomas, *Chem. Soc. Rev.*, 2010, **39**, 165–173; (*d*) M. J. Stanford and A. P. Dove, *Chem. Soc. Rev.*, 2010, **39**, 486–494; (*e*) K. Fukushima and Y. Kimura, *Polym. Int.*, 2006, **55**, 626–642.

7 (*a*) H. A. Brown and R. M. Waymouth, *Acc. Chem. Res.*, 2013, **46**, 2585–2596; (*b*) N. E. Kamber, W. Jeong, R. M. Waymouth, R. C. Pratt, B. G. G. Lohmeijer and J. L. Hedrick, *Chem. Rev.*, 2007, **107**, 5813–5840.

8 (*a*) A. K. Sutar, T. Maharana, S. Dutta, C. T. Chen and C. C. Lin, *Chem. Soc. Rev.*, 2010, **39**, 1724–1746; (*b*) C. A. Wheaton, P. G. Hayes and B. J. Ireland, *Dalton Trans.*, 2009, 4832–4846; (*c*) H. R. Kricheldorf, *Chem. Rev.*, 2009, **109**, 5579–5594; (*d*) T. Chivers and J. Konu, *Comments Inorg. Chem.*, 2009, **30**, 131–176.

9 (*a*) A. Stopper, J. Okuda and M. Kol, *Macromolecules*, 2012, **45**, 698–704; (*b*) R. Heck, E. Schulz, J. Collin and J. F. Carpentier, *J. Mol. Catal. A: Chem.*, 2007, **268**, 163–168; (*c*) P. L. Arnold, J. C. Buffet, R. Blaudeck, S. Sujecki and C. Wilson, *Chem.–Eur. J.*, 2009, **15**, 8241–8250; (*d*) P. L. Arnold, J. C. Buffet, R. P. Blaudeck, S. Sujecki, A. J. Blake and C. Wilson, *Angew. Chem., Int. Ed.*, 2008, **47**, 6033–6036; (*e*) A. Otero, J. Fernandez-Baeza, A. Lara-Sanchez, C. Alonso-Moreno, I. Marquez-Segovia, L. F. Sanchez-Barba and A. M. Rodriguez, *Angew. Chem., Int. Ed.*, 2009, **48**, 2176–2179; (*f*) M. Normand, E. Kirillov, T. Roisnel and J. F. Carpentier, *Organometallics*, 2012, **31**, 1448–1457; (*g*) F. Drouin, T. J. J. Whitehorne and F. Schaper, *Dalton Trans.*, 2011, **40**, 1396–1400; (*h*) J.-C. Buffet, J. Okuda and P. L. Arnold, *Inorg. Chem.*, 2010, **49**, 419–426; (*i*) A. Buchard, D. R. Carbery, M. G. Davidson, P. K. Ivanova, B. J. Jeffery, G. I. Kociok-Kohn and J. P. Lowe, *Angew. Chem., Int. Ed.*, 2014, **53**, 13858–13861; (*j*) A. P. Dove, H. B. Li, R. C. Pratt, B. G. G. Lohmeijer, D. A. Culkin, R. M. Waymouth and J. L. Hedrick, *Chem. Commun.*, 2006, 2881–2883; (*k*) L. Zhang, F. Nederberg, R. C. Pratt, R. M. Waymouth, J. L. Hedrick and C. G. Wade, *Macromolecules*, 2007, **40**, 4154–4158; (*l*) H. L. Chen, S. Dutta, P. Y. Huang and C. C. Lin, *Organometallics*, 2012, **31**, 2016–2025; (*m*) H. B. Wang, Y. Yang and H. Y. Ma, *Macromolecules*, 2014, **47**, 7750–7764; (*n*) Isotacticity can be quantified by the probability of meso linkages (P_m) in the polymer. A completely isotactic polymer would have $P_m = 1$.

10 (*a*) G. Montaudo, M. S. Montaudo, C. Puglisi, F. Samperi, N. Spassky, A. LeBorgne and M. Wisniewski, *Macromolecules*, 1996, **29**, 6461–6465; (*b*) N. Spassky, M. Wisniewski, C. Pluta and A. LeBorgne, *Macromol. Chem. Phys.*, 1996, **197**, 2627–2637; (*c*) T. M. Ovitt and G. W. Coates, *J. Polym. Sci., Part A: Polym. Chem.*, 2000, **38**, 4686–4692; (*d*) D. Jhurry, A. Bhaw-Luximon and N. Spassky, *Macromol. Symp.*, 2001, **175**, 67–79; (*e*) Z. Y. Zhong, P. J. Dijkstra and J. Feijen, *Angew. Chem., Int. Ed.*, 2002, **41**, 4510–4513; (*f*) Z. Y. Zhong, P. J. Dijkstra and J. Feijen, *J. Am. Chem. Soc.*, 2003, **125**, 11291–11298; (*g*) Z. H. Tang, X. S. Chen, X. Pang, Y. K. Yang, X. F. Zhang and X. B. Jing, *Biomacromolecules*, 2004, **5**, 965–970; (*h*) Z. H. Tang, X. S. Chen, Y. K. Yang, X. Pang, J. R. Sun, X. F. Zhang and X. B. Jing, *J. Polym. Sci., Part A: Polym. Chem.*, 2004, **42**, 5974–5982; (*i*) N. Nomura, R. Ishii, M. Akakura and K. Aoi, *J. Am. Chem. Soc.*, 2002, **124**, 5938–5939; (*j*) R. Ishii, N. Nomura and T. Kondo, *Polym. J.*, 2004, **36**, 261–264; (*k*) N. Nomura, R. Ishii, Y. Yamamoto and T. Kondo, *Chem.–Eur. J.*, 2007, **13**, 4433–4451; (*l*) N. Nomura, A. Akita, R. Ishii and M. Mizuno, *J. Am. Chem. Soc.*, 2010, **132**, 1750–1751; (*m*) P. Hormnirun, E. L. Marshall, V. C. Gibson, A. J. P. White and D. J. Williams, *J. Am. Chem. Soc.*, 2004, **126**, 2688–2689; (*n*) P. Hormnirun, E. L. Marshall, V. C. Gibson, R. I. Pugh and A. J. P. White, *Proc. Natl. Acad. Sci. U. S. A.*, 2006, **103**, 15343–15348; (*o*) M. H. Chisholm, N. J. Patmore and Z. P. Zhou, *Chem. Commun.*, 2005, 127–129; (*p*) M. H. Chisholm, J. C. Gallucci, K. T. Quisenberry and Z. P. Zhou, *Inorg. Chem.*, 2008, **47**, 2613–2624; (*q*) H. Z. Du, A. H. Velders, P. J. Dijkstra, J. R. Sun, Z. Y. Zhong, X. S. Chen and J. Feijen, *Chem.–Eur. J.*, 2009, **15**, 9836–9845; (*r*) H. Z. Du, A. H. Velders, P. J. Dijkstra, Z. Y. Zhong, X. S. Chen and J. Feijen, *Macromolecules*, 2009, **42**, 1058–1066; (*s*) N. Maudoux, T. Roisnel, V. Dorcet, J. F. Carpentier and Y. Sarazin, *Chem.–Eur. J.*, 2014, **20**, 6131–6147; (*t*) A. Pilone, K. Press, I. Goldberg, M. Kol, M. Mazzeo and M. Lamberti, *J. Am. Chem. Soc.*, 2014, **136**, 2940–2943.

11 (*a*) C. Bakewell, T. P. A. Cao, N. Long, X. F. Le Goff, A. Auffrant and C. K. Williams, *J. Am. Chem. Soc.*, 2012, **134**, 20577–20580; (*b*) C. Bakewell, A. J. P. White, N. J. Long and C. K. Williams, *Angew. Chem., Int. Ed.*, 2014, **53**, 9226–9230.

12 (*a*) D. C. Aluthge, B. O. Patrick and P. Mehrkhodavandi, *Chem. Commun.*, 2013, **49**, 4295–4297; (*b*) D. C. Aluthge, E. X. Yan, J. M. Ahn and P. Mehrkhodavandi, *Inorg. Chem.*, 2014, **53**, 6828–6836.

13 (*a*) S. M. Quan and P. L. Diaconescu, *Chem. Commun.*, 2015, **51**, 9643–9646; (*b*) S. Ghosh, R. R. Gowda, R. Jagan and D. Chakraborty, *Dalton Trans.*, 2015, **44**, 10410–10422; (*c*) M. Normand, V. Dorcet, E. Kirillov and J. F. Carpentier, *Organometallics*, 2013, **32**, 1694–1709; (*d*) A. Kapelski and J. Okuda, *J. Polym. Sci., Part A: Polym. Chem.*, 2013, **51**, 4983–4991; (*e*) L. E. N. Allan, G. G. Briand, A. Decken,

J. D. Marks, M. P. Shaver and R. G. Wareham, *J. Organomet. Chem.*, 2013, **736**, 55–62; (*f*) E. M. Broderick, N. Guo, C. S. Vogel, C. Xu, J. Sutter, J. T. Miller, K. Meyer, P. Mehrkhodavandi and P. L. Diaconescu, *J. Am. Chem. Soc.*, 2011, **133**, 9278–9281; (*g*) M. Bompart, J. Vergnaud, H. Strub and J. F. Carpentier, *Polym. Chem.*, 2011, **2**, 1638–1640; (*h*) M. P. Blake, A. D. Schwarz and P. Mountford, *Organometallics*, 2011, **30**, 1202–1214; (*i*) A. Pietrangelo, S. C. Knight, A. K. Gupta, L. J. Yao, M. A. Hillmyer and W. B. Tolman, *J. Am. Chem. Soc.*, 2010, **132**, 11649–11657; (*j*) M. G. Hu, M. Wang, P. L. Zhang, L. Wang, F. J. Zhu and L. C. Sun, *Inorg. Chem. Commun.*, 2010, **13**, 968–971; (*k*) A. Pietrangelo, M. A. Hillmyer and W. B. Tolman, *Chem. Commun.*, 2009, 2736–2737; (*l*) I. Peckermann, A. Kapelski, T. P. Spaniol and J. Okuda, *Inorg. Chem.*, 2009, **48**, 5526–5534.

14 S. Dagorne, M. Normand, E. Kirillov and J. F. Carpentier, *Coord. Chem. Rev.*, 2013, **257**, 1869–1886.

15 (*a*) A. F. Douglas, B. O. Patrick and P. Mehrkhodavandi, *Angew. Chem., Int. Ed.*, 2008, **47**, 2290–2293; (*b*) C. Xu, I. Yu and P. Mehrkhodavandi, *Chem. Commun.*, 2012, **48**, 6806–6808; (*c*) I. Yu, A. Acosta-Ramirez and P. Mehrkhodavandi, *J. Am. Chem. Soc.*, 2012, **134**, 12758–12773; (*d*) D. C. Aluthge, C. L. Xu, N. Othman, N. Noroozi, S. G. Hatzikiriakos and P. Mehrkhodavandi, *Macromolecules*, 2013, **46**, 3965–3974; (*e*) J. Fang, I. Yu, P. Mehrkhodavandi and L. Maron, *Organometallics*, 2013, **32**, 6950–6956.

16 (*a*) B. J. O'Keefe, L. E. Breyfogle, M. A. Hillmyer and W. B. Tolman, *J. Am. Chem. Soc.*, 2002, **124**, 4384–4393; (*b*) B. J. O'Keefe, S. M. Monnier, M. A. Hillmyer and W. B. Tolman, *J. Am. Chem. Soc.*, 2001, **123**, 339–340; (*c*) C. K. Williams, L. E. Breyfogle, S. K. Choi, W. Nam, V. G. Young, M. A. Hillmyer and W. B. Tolman, *J. Am. Chem. Soc.*, 2003, **125**, 11350–11359; (*d*) B. M. Chamberlain, M. Cheng, D. R. Moore, T. M. Ovitt, E. B. Lobkovsky and G. W. Coates, *J. Am. Chem. Soc.*, 2001, **123**, 3229–3238; (*e*) C. K. Williams, N. R. Brooks, M. A. Hillmyer and W. B. Tolman, *Chem. Commun.*, 2002, 2132–2133; (*f*) R. H. Platel, L. M. Hodgson, A. J. P. White and C. K. Williams, *Organometallics*, 2007, **26**, 4955–4963; (*g*) H. Y. Ma, T. P. Spaniol and J. Okuda, *Angew. Chem., Int. Ed.*, 2006, **45**, 7818–7821; (*h*) A. Duda and S. Penczek, *Makromol. Chem., Macromol. Symp.*, 1991, **47**, 127–140.

17 M. H. Chisholm, J. Gallucci and K. Phomphrai, *Inorg. Chem.*, 2002, **41**, 2785–2794.

18 (*a*) K. M. Osten, I. Yu, I. R. Duffy, P. O. Lagaditis, J. C. C. Yu, C. J. Wallis and P. Mehrkhodavandi, *Dalton Trans.*, 2012, **41**, 8123–8134; (*b*) K. M. Osten, D. C. Aluthge, B. O. Patrick and P. Mehrkhodavandi, *Inorg. Chem.*, 2014, **53**, 9897–9906; (*c*) K. M. Osten, D. C. Aluthge and P. Mehrkhodavandi, *Dalton Trans.*, 2015, **44**, 6126–6139.

19 (*a*) E. N. Jacobsen, W. Zhang and M. L. Guler, *J. Am. Chem. Soc.*, 1991, **113**, 6703–6704; (*b*) X. Q. Yao, M. Qiu, W. R. Lu, H. L. Chen and Z. Zheng, *Tetrahedron: Asymmetry*, 2001, **12**, 197–204; (*c*) V. Rudzevich, D. Schollmeyer, D. Braekers, J. F. Desreux, R. Diss, G. Wipff and V. Bohmer, *J. Org. Chem.*, 2005, **70**, 6027–6033; (*d*) C. T. Cohen, C. M. Thomas, K. L. Peretti, E. B. Lobkovsky and G. W. Coates, *Dalton Trans.*, 2006, 237–249.

20 (*a*) D. A. Atwood, J. A. Jegier and D. Rutherford, *Inorg. Chem.*, 1996, **35**, 63–70; (*b*) T. M. Ovitt and G. W. Coates, *J. Am. Chem. Soc.*, 2002, **124**, 1316–1326.

21 D. A. Atwood and M. J. Harvey, *Chem. Rev.*, 2001, **101**, 37–52.

22 (*a*) D. A. Atwood, J. A. Jegier and D. Rutherford, *Bull. Chem. Soc. Jpn.*, 1997, **70**, 2093–2100; (*b*) M. S. Hill and D. A. Atwood, *Main Group Chem.*, 1998, **2**, 191–202.

23 The ^{1}H NMR spectra of incomplete reactions, after the addition of NaOEt show resonances corresponding to the respective characterized (ONNO$_{R}$)InCl complexes, indicating their synthesis as an intermediate species (Fig. S28†).

24 J. W. Yoon, T. S. Yoon and W. Shin, *Acta Crystallogr., Sect. C: Cryst. Struct. Commun.*, 1997, **53**, 1685–1687.

25 F. A. Bovey and P. A. Mirau, *NMR of Polymers*, Academic Press, San Diego, 1996.

26 (*a*) J. Coudane, C. Ustariz-Peyret, G. Schwach and M. Vert, *J. Polym. Sci., Part A: Polym. Chem.*, 1997, **35**, 1651–1658; (*b*) M. T. Zell, B. E. Padden, A. J. Paterick, K. A. M. Thakur, R. T. Kean, M. A. Hillmyer and E. J. Munson, *Macromolecules*, 2002, **35**, 7700–7707.

27 (*a*) H. R. Kricheldorf, C. Boettcher and K. U. Tonnes, *Polymer*, 1992, **33**, 2817–2824; (*b*) A. M. Goldys and D. J. Dixon, *Macromolecules*, 2014, **47**, 1277–1284; (*c*) T. R. Jensen, L. E. Breyfogle, M. A. Hillmyer and W. B. Tolman, *Chem. Commun.*, 2004, 2504–2505.

28 P. Mehrkhodavandi, D. C. Aluthge, T. J. Clark, B. Mariampillai and Y. Yan, *Ca. Pat.*, PCT/CA2013/050191, 2013.

29 P. Mehrkhodavandi and D. C. Aluthge, *Ca. Pat.*, PCT/CA2015/050601, 2014.

